

# Mechanical properties of zirconia-based ceramics as functions of temperature

M.J. Andrews<sup>a,\*</sup>, M.K. Ferber<sup>b</sup>, E. Lara-Curzio<sup>b</sup>

<sup>a</sup>Advanced Materials Technology, Caterpillar Inc., Peoria, IL 61656-1875, USA

<sup>b</sup>Metals and Ceramics Division, Oak Ridge National Laboratory, Oak Ridge TN 37830-6069, USA

Received 22 November 2001; accepted 20 March 2002

## Abstract

Commercially available ceramics, MgO–ZrO<sub>2</sub>, CeO<sub>2</sub>–ZrO<sub>2</sub>, and an in-house fabricated zirconia-toughened mullite were examined in this study for use as a structural component in diesel engines. The fast fracture strengths of these materials were measured by loading ASTM C-1161-B specimens in four-point flexure at 30 MPa/s and at 20, 200, 400, 600, and 850 °C. The dynamic fatigue or slow crack growth susceptibility was assessed at 20 and 850 °C by combining the fast fracture strengths with strength data obtained by testing the same specimens in four-point flexure at 0.30 and 0.003 MPa/s stressing rates, as specified in the ASTM C 1368 standard. Fracture toughness was measured following the ASTM C-1421 standard and using chevron notch specimens in three-point flexure at room and elevated temperatures. The strength of the zirconia-toughened mullite was invariant to increases in the temperature and decreases in the loading rate, while the MgO–ZrO<sub>2</sub> and CeO<sub>2</sub>–ZrO<sub>2</sub> materials exhibited strength degradation as temperatures increased and the loading rates decreased. Temperature was observed to have the greatest influence on fracture toughness. As temperatures increased, the fracture toughness values dramatically decreased for all the materials examined in this study. Improvements in the fracture toughness are needed most for these ceramic materials in order to meet the structural requirements and to develop a more durable and reliable diesel engine component. © 2002 Elsevier Science Ltd. All rights reserved.

**Keywords:** Fatigue; Fracture; CeO<sub>2</sub>–ZrO<sub>2</sub>; MgO–ZrO<sub>2</sub>

## 1. Introduction

Meeting stringent diesel emission regulations will likely incorporate ceramic materials that provide better thermal management to utilize more of the unused thermal energy from combustion. The thermal efficiency of the diesel engine is mainly dependent on the operating temperatures where higher combustion temperatures provide greater energy efficiency. Raising the combustion temperature of diesel engines is also known to increase NO<sub>x</sub>, and thus an optimal temperature must be identified that increases the thermal efficiency while minimizing the NO<sub>x</sub>. Introducing insulating ceramic materials in the diesel engine combustion chamber can provide greater control in maintaining the optimal operating conditions, and a better means to manage the unused thermal energy. The advantage of improving

engine efficiency is realized in lower fuel costs, the greatest expenditure that the consumer pays to operate on-highway diesel powered trucks.<sup>1</sup>

Ceramic materials having low thermal conductivity and high fracture toughness were examined in this study for use as a structural insulating cylinder head insert, a component that is illustrated in Fig. 1. Zirconia-based ceramic materials are well documented for low thermal conductivity, high fracture toughness, as well as offering excellent corrosion and wear resistance in adverse environments.<sup>2</sup> Previous studies have demonstrated significant increases in energy efficiency by using insulating materials in the combustion chamber.<sup>1</sup> The objective of this study is to examine several zirconia-based ceramic materials that have low thermal conductivity, and that also possess high strength and fracture toughness at elevated temperatures. Candidate materials must maintain structural stability in adverse diesel environments, and must demonstrate quantifiable improvements in performance, durability, and reliability in order to justify any increase in component cost.

\* Corresponding author. Tel.: +1-309-578-3896; fax: +1-309-578-2953.

E-mail address: andrews\_mark\_j@cat.com (M.J. Andrews).

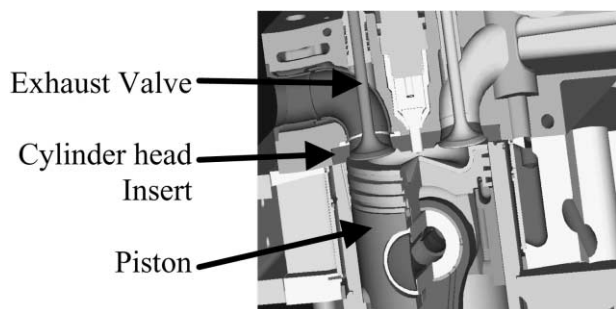


Fig. 1. Schematic of internal combustion engine showing the location of the cylinder head insert component.

## 2. Experimental methods

### 2.1. Material selection and preparation

Zirconia-based ceramics were identified for this study due to their low thermal conductivity (2–4 W/m K), high strength at elevated temperatures (650–800 MPa) and high fracture toughness (8–12 MPa m<sup>1/2</sup>) through transformation toughening, as reported in the literature.<sup>1</sup> These published mechanical properties meet the design criteria for the cylinder head insert component. Previous to this program, Caterpillar had developed a processing, microstructural, and mechanical property

relationship for an in-house fabricated zirconia toughened mullite, designated as ZTM. This material demonstrated the low thermal conductivity and stability needed in a diesel engine environment. Cost effective processing methods for fabricating ZTM production components were also identified. Initially, stabilized zirconia ceramics such as MgO–ZrO<sub>2</sub>, CeO<sub>2</sub>–ZrO<sub>2</sub> were not considered for the study due to their reported strength loss from exposure to high temperature, moist environments. The investigators chose to include commercially available stabilized zirconia ceramics later in the study after processing changes were made to improve the strength retention at elevated temperatures.

Magnesium stabilized zirconia, designated as Mg-TTZ, and two Cerium stabilized zirconias, designated as Ce-TZP, were selected from CoorsTek in Golden, CO and CoorsTek and Ferro Corp., of Shreve OH, respectively. Typical microstructures of these materials are shown in Fig. 2. The magnesium-stabilized zirconia has a grain structure on the order of 50–100 µm, while both cerium-stabilized zirconias have a grain structure on the order of 2–5 µm. The zirconia-toughened mullite has a finer grain structure on the order of 0.2–1.0 µm.

As-received materials were fabricated into flexure bars having a rectangular cross-section and the nominal dimensions of 3×4×50 mm. The flexure test specimens were machined using the conventional practiced

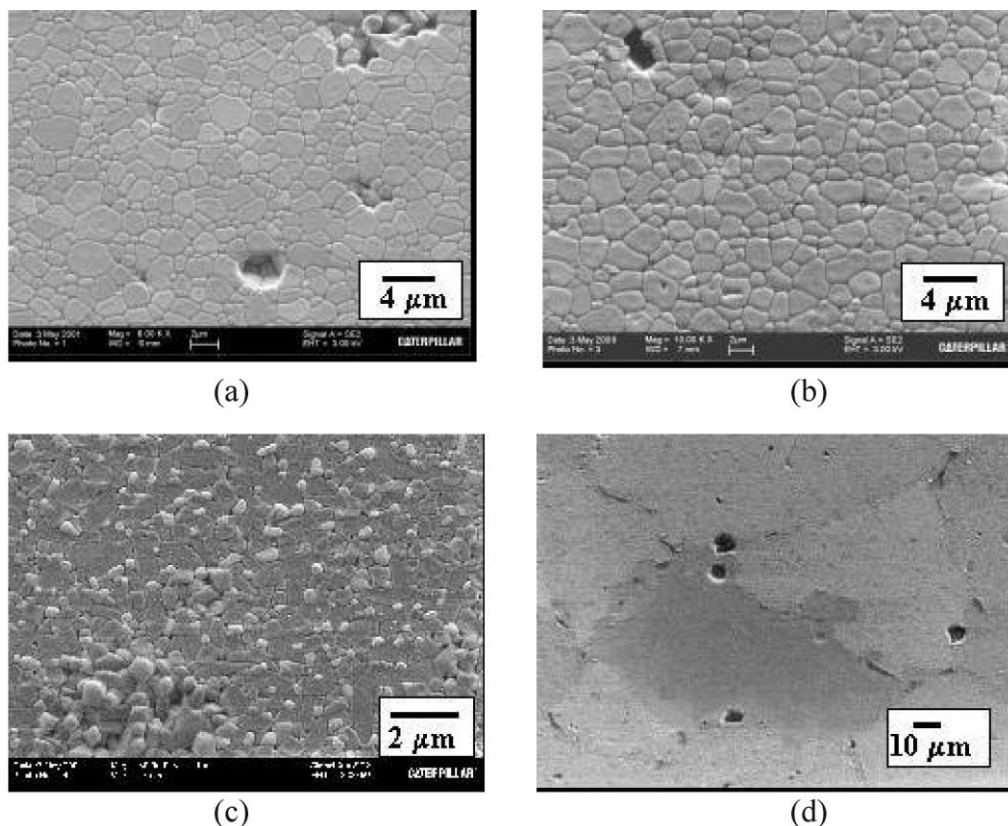


Fig. 2. Photomicrographs illustrating the microstructure of the materials in this study. Ce-TZP CoorsTek (a), Ce-TZP Ferro (b), ZTM (c) and Mg-TTZ (d). The large dark region in (d) is a single grain.

machining procedures as found in the ASTM C-1161-B standard.<sup>3</sup> The final grinding was completed using a 320-diamond grit wheel, and the edges of the bars were chamfered to reduce the likelihood of corner-induced failures. A portion of machined flexure bars designated for fracture toughness tests were notched with a diamond blade at the center of the bar, as specified in the ASTM C-1421 standard.<sup>4</sup>

## 2.2. Test facilities and procedures

The specimens were tested at the High Temperature Materials Laboratory (HTML) located within the Oak Ridge National Laboratory (ORNL) complex, Oak Ridge, TN, through a Facility User Program. The test facilities consisted of a Flexure Test System (FTS), an in-house test machine designed by the ORNL technical staff. The FTS is capable of testing three flexure specimens simultaneously at ambient and elevated temperatures. Each system included a CM furnace (Rapid Temp Furnace, Model 870121, Bloomfield, NJ) permitting temperatures up to 1600 °C. Keithly closed-loop control and data acquisition software (Soft500, Cleveland, OH) on a PC computer controlled and monitored the loading rates and temperature. The rate of loading was programmed using the Soft500 software. Table 1 summarizes the number of test specimens used for the fast fracture, dynamic fatigue, and fracture toughness tests.

Fast fracture and dynamic fatigue test specimens were positioned in a semiarticulating four-point flexure fixture made from  $\alpha$ -SiC and then placed inside the CM furnaces between two opposed and concentrically aligned  $\alpha$ -SiC rods. The top rod applied

the load generated using a pneumatically drive air cylinder while the bottom rod was attached to a load cell. Displacement was measured using a linear variable displacement transducer.

Calculations of the test specimen strength followed the ASTM C-1239 standard<sup>5</sup> and were done using the computer code CERAMIC developed by Honeywell (formerly AlliedSignal Engines, Inc., Phoenix, AZ).<sup>6</sup> This computer code uses the two-parameter Weibull distribution for the estimating the characteristic strength of the data, and the modulus, which is a measure of the data variance. Confidence limits for the data were estimated using likelihood ratio statistics, and details of this method are described elsewhere.<sup>6</sup>

Fracture toughness test specimens were loaded in three-point flexure using the same test facilities. The bottom half of the flexure fixture was used to position and support the chevron notch specimen and the load was applied using a  $\alpha$ -SiC rod that had a chisel point end machined into its end. At each test temperature, the compliance of the machine's load train assembly was measured, and this data was subtracted from the test specimen load-displacement data before calculating the fracture toughness,  $K_{IC}$ . Dimensional measurements of the chevron notch were made after fracture and using an optical comparator (Model V-12, Nikon, Melville, NY). Equations for calculating the fracture toughness taken from the ASTM 1368 standard<sup>7</sup> were programmed into a LabView software (Version 2.2.1, Austin, TX) routine. The fracture toughness was calculated using the load displacement data, the compliance data, the dimensional measurements of the chevron notch, and the elastic properties of each ceramic material.

Table 1

Number of test specimens and the test conditions examined in this study

Stressing rate (MPa/s) Temperature (°C)	Caterpillar ZTM	CoorsTek Mg-TTZ	CoorsTek Ce-TZP	Ferro Ce-TZP
<i>Fast fracture</i>				
30 MPa/s 20 °C	10	10	10	7
30 MPa/s 200 °C	10	10	7	6
30 MPa/s 400 °C	10	10	7	6
30 MPa/s 600 °C	10	10	7	6
30 MPa/s 850 °C	10	10	7	6
<i>Dynamic fatigue</i>				
0.30 MPa/s 20 °C	10	10	10	7
0.30 MPa/s 850 °C	11	10	10	7
0.0030 MPa/s 20 °C	10	9	10	7
0.0030 MPa/s 850 °C	9	10	8	7
<i>Fracture toughness</i>				
0.005 mm/s 20 °C	10	10	10	—
0.005 mm/s 200 °C	—	7	7	—
0.005 mm/s 400 °C	—	8	7	—
0.005 mm/s 600 °C	—	8	7	—
0.005 mm/s 850 °C	9	7	5	—

## 3. Results

### 3.1. Fast fracture results

Presented in Fig. 3 are the characteristic strength estimates for the ZTM and the Mg-TTZ ceramic materials tested at 30 MPa/s and at 20, 200, 400, 600, and 850 °C. The boxed region at the top of each column represents the 95% confidence bounds for each data.

In Fig. 3, the ZTM shows a slight decrease in strength as test temperatures increased with only one significant decrease over the entire temperature range. The Mg-TTZ shows significant decreases in strengths in the 20–600 °C range but equivalent strengths at 600 and 850 °C. By comparing the 95% confidence boundaries for each data in Fig. 3, the Mg-TTZ shows a smaller variance in the strength data than the ZTM material.

In Fig. 4 the characteristic strengths for the two Ce-TZP materials are presented as a function of temperature. Both materials show significant strength decreases as temperature increase, the same trend observed with

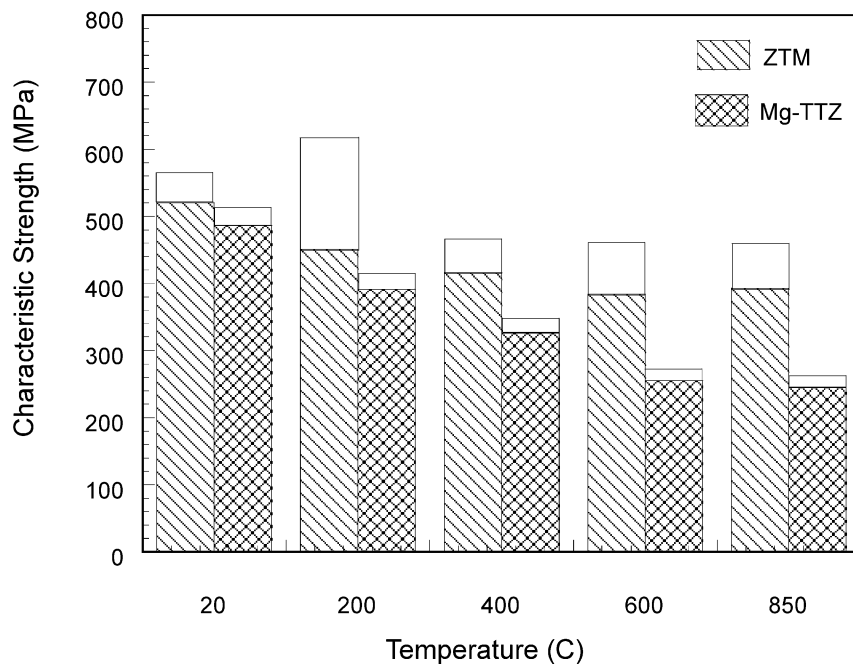


Fig. 3. Fast fracture strength as a function of temperature for ZTM and Mg-TTZ materials. The boxed zone above each column represents the 95% confidence region of the data.

the Mg-TTZ material. For the CoorsTek Ce-TZP material, the strength significantly decreases between 20 and 600 °C, and between 600 and 850 °C, the strengths are statistically equivalent at a 95% confidence level. This same trend is also observed with the Ferro Ce-TZP but occurring at lower strength values. In Fig. 4 the variance in strength data appears larger for the CoorsTek Ce-TZP than for the Ferro Ce-TZP.

### 3.2. Dynamic fatigue results

Fig. 5 presents the 20 °C dynamic fatigue or slow crack growth results for all of the ceramic materials examined in this study. At a 95% confidence level, the ZTM showed no strength degradation as the loading rate decreased from 30 to 0.30 MPa/s, and then from 0.30 to 0.003 MPa/s. The Mg-TTZ and the Ce-TZP

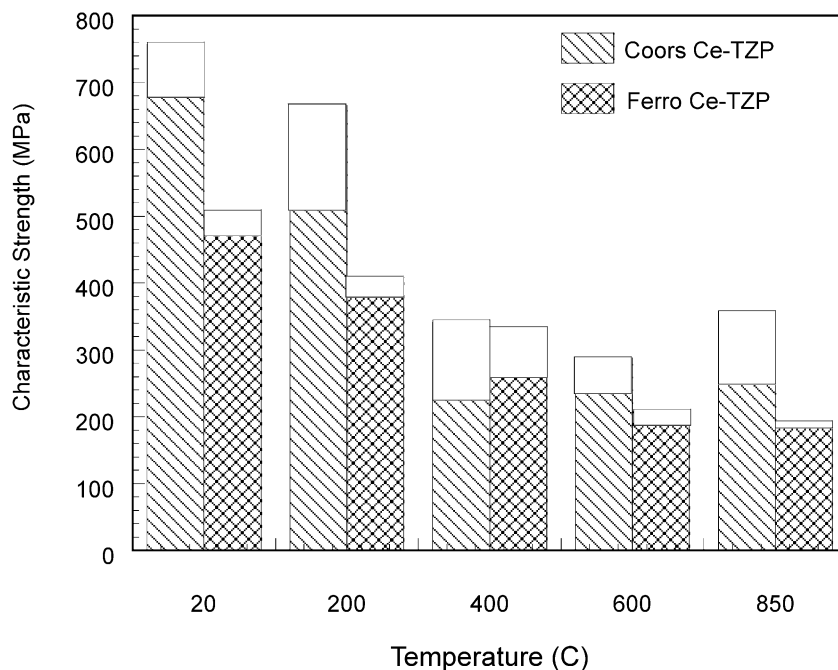


Fig. 4. Fast fracture strength as a function of temperature for two Ce-TZP materials. The boxed zone above each column represents the 95% confidence region of the data.

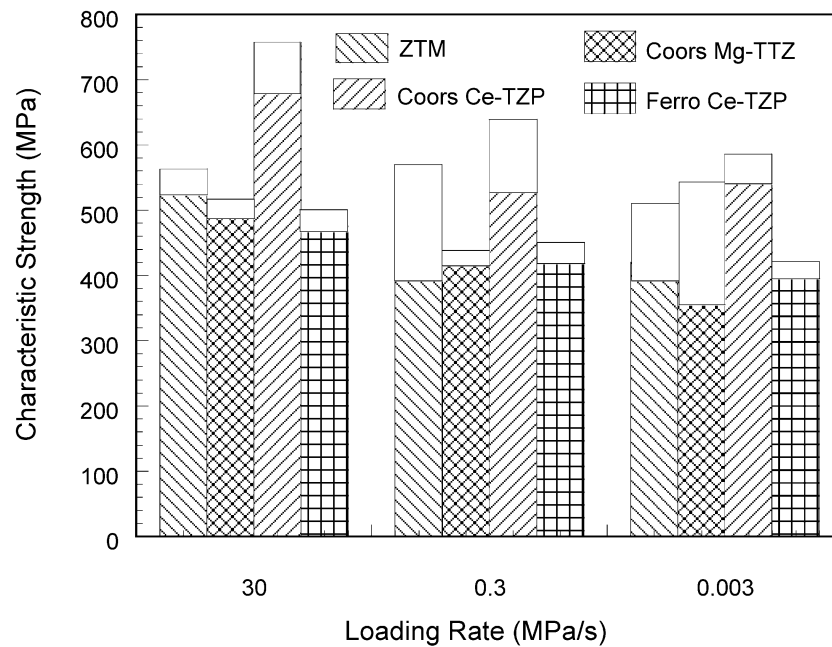


Fig. 5. Strength as a function of stressing rate at 20 °C. The boxed zone above each column represents the 95% confidence region of the data.

materials show a significant decrease in strength as the stressing rate decreased between 30 and 0.30 MPa/s while the strengths are statistically equivalent between 0.30 and 0.003 MPa/s. The exception to this observation was the Ferro Ce-TZP that showed a significant decrease in strength at all stressing rates. The lowest variance in strength data is observed with the Ferro Ce-TZP material.

Fig. 6 illustrates the dynamic fatigue results for the ceramic materials tested at 850 °C. Comparing Fig. 6

with Fig. 5 indicates that an overall decrease in strength occurs when testing at 850 °C. The ZTM shows no strength degradation as the stressing rate decreases while the Mg-TTZ shows an increase in strength as the stressing rate decreases, and at a 95% confidence level, this increase in strength is significant between 30 and 0.003 MPa/s. The CoorsTek Ce-TZP and the Ferro Ce-TZP materials each show a significant decrease in strength when the stressing rate decreases from 30 to 0.30 MPa/s, but maintain this strength when tested at

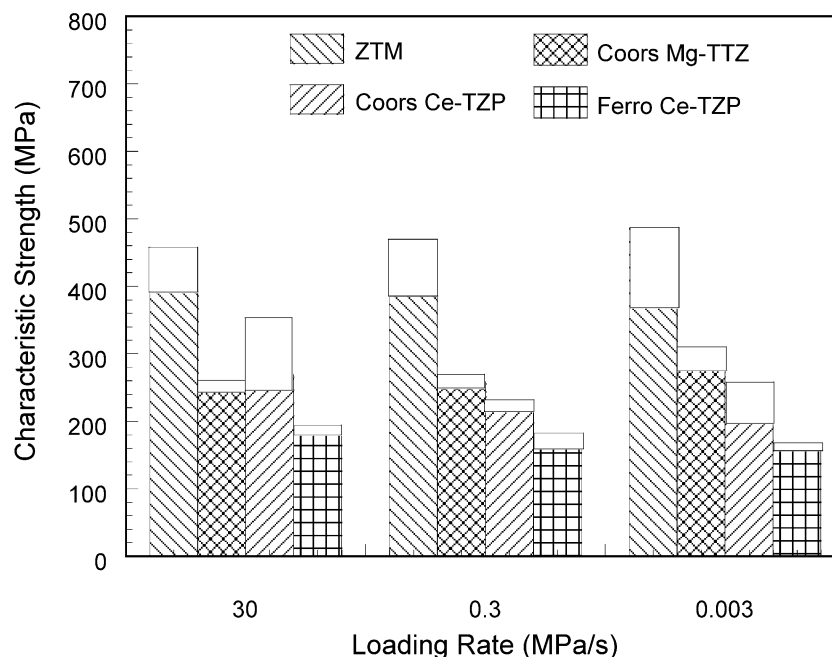


Fig. 6. Strength as a function of stressing rate at 850 °C. The boxed zone above each column represents the 95% confidence region of the data.

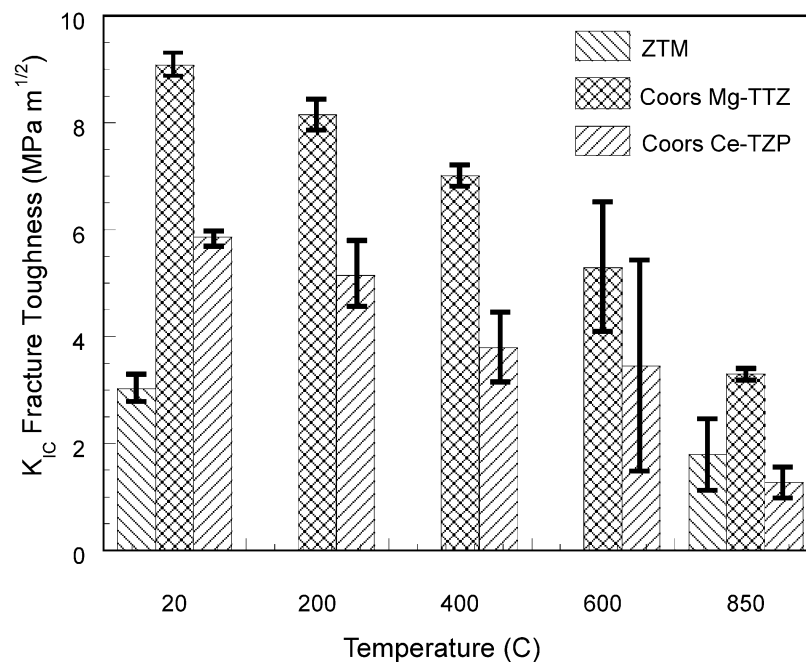


Fig. 7. Fracture toughness as a function of temperature. The standard deviation of the data is represented with interval bars at the end of each column.

the 0.003 MPa/s rate. The CoorsTek Mg-TTZ and the Ferro Ce-TZP show the least variance in strength data at 850  $^{\circ}\text{C}$ .

### 3.3. Fracture toughness results

The fracture toughness of select zirconia materials as a function of temperature using chevron notch specimens is illustrated in Fig. 7. Located at the top of each column are bars representing the data standard deviation.

Fig. 7 shows that fracture toughness significantly decreases as the temperature increases for all materials examined in the study. Scatter in the data show that several toughness values for each material are equivalent within a standard deviation but are not equivalent at the extreme temperatures of 20 and 850  $^{\circ}\text{C}$ . A 40% decrease in fracture toughness was observed with the ZTM material when tested at 20 and 850  $^{\circ}\text{C}$ , while the fracture toughness of Mg-TTZ and the CoorsTek Ce-TZP decreased approximately 64 and 78%, respectively, over the same temperature range.

## 4. Discussion

The study illustrates different ways that zirconia ceramics are used to improve strength and fracture toughness through stress induced transformation toughening. The CoorsTek Mg-TTZ material is known as precipitation-toughened ceramic in which a stabilizing compound retains cubic grains after sintering and the tetragonal phase is precipitated within the cubic

grain typically by an aging process. The CoorsTek and Ferro Ce-TZP materials are considered as a single-phase tetragonal solid solution, where the processing objective is to retain as many tetragonal grains upon cooling. Lastly, the ZTM is a dispersion-toughened ceramic where tetragonal zirconia grains are distributed within the mullite for enhancing fracture toughness and strength. Strength and fracture toughness properties are determined through a variety of processing controls such as composition, aging, and tetragonal particle size. The critical size of the tetragonal precipitates or grains and the temperature at which constrained precipitates transform from tetragonal to monoclinic are usually attributed to the material's thermal processing history.

The fracture toughness (Fig. 7) was shown to depend on temperature such that when the temperatures increase, the fracture toughness values decrease. These results agree with several previous published studies on transformation toughening zirconias. The scatter in the fracture toughness data is shown to also increase as the temperatures increase. At 600  $^{\circ}\text{C}$ , the CoorsTek Mg-TTZ and Ce-TZP reach a maximum variance of  $\pm 1.2$  and  $\pm 2.0 \text{ MPa m}^{1/2}$ , respectively. At all other temperatures the variance in the data is at least 50% smaller than these maximum values. As temperatures increase, the decrease in fracture toughness is likely due to a decrease in the free energy of transformation,<sup>2</sup> the energy that is responsible for improving strength and toughness properties. The high variance in the fracture toughness data at one temperature suggests that this critical temperature where no phase transformation occurs may be around 600  $^{\circ}\text{C}$  for both materials.

The ZTM was tested only at 20 and 850 °C, and the scatter in this fracture toughness data appears to follow the same trend as observed with the CoorsTek materials. The fracture toughness values for the ZTM ranged from 1.8 to 3.0 MPa m<sup>1/2</sup> while the fracture toughness of pure mullite is approximately 1.6 MPa m<sup>1/2</sup>. This finding suggests that transformation toughening was able to nearly double the fracture toughness property at 20 °C, and had little influence at 850 °C.

The study showed that the strength of the ZTM was not influenced by temperature and loading rate, while the other materials illustrated a strength dependency from both parameters. The flexure strength of the CoorsTek Mg-TTZ, Ce-TZP, and the Ferro Ce-TZP is shown to monotonically decrease with increasing temperatures until reaching the 400–600 °C temperature range, as shown in Fig. 4. From this temperature range and above, the flexure strength for these materials appear to stabilize. The dynamic fatigue data (Figs. 5 and 6) show that the CoorsTek and Ferro materials are much more susceptible to slow crack growth at 850 °C than at 20 °C. These observations suggest that the fast fracture and slow crack growth data may also support the notion of a temperature limit where no transformation occurs is somewhere around 600 °C for these materials.

One might anticipate that the mechanical properties for the CoorsTek and Ferro Ce-TZP would be similar since the grain sizes of each material are approximately 2–5 µm, see Fig. 2. Perhaps due to compositional differences, the Ferro Ce-TZP was always found to have flexure strength approximately 15–35% lower than the CoorsTek Ce-TZP, regardless of test temperature.

The number of test specimens for each test condition ranged from 6 to 11 and having a greater number of test specimens would likely reduce the variance observed with ZTM and CoorsTek Ce-TZP materials. However, it is believed that additional test data would not significantly alter the trends observed in this study. The Ferro Ce-TZP provided the lowest variance in nearly all test conditions despite the smaller than average sample size (7), as shown in Table 1.

## 5. Conclusions

The strength of the materials showed a greater sensitivity to temperature increases than to stressing rate decreases. Without performing extensive phase identification analyses, the combined results from the fast fracture, dynamic fatigue, and fracture toughness data suggest a means to identify transformation temperature limit. By identifying this temperature, component performance requirements can be compared with material performance in order to assess design, reliability, and

durability issues. Regardless of processing technique, the Mg-TTZ and the Ce-TZP both exhibit the same transformation temperature limitation

The ZTM was found to be the most stable over the 20–850 °C range of interest but lacked in having adequate fracture toughness. The materials examined in this study did not meet all of the design requirements of the cylinder insert component, particularly with regard to fracture toughness at elevated temperatures. Processing improvements to increase the critical transformation temperature limit may increase the fracture toughness and strength values at elevated temperatures, which are needed to utilize ceramic materials in a diesel engine.

## Acknowledgements

This Research was sponsored in part by the Assistant Secretary for Energy Efficiency and Renewable Energy, Office of Transportation Technologies as part of the High Temperature Materials Laboratory User Program, Oak Ridge National Laboratory, managed by UT-Battelle Corp. for the US Department of Energy under contract DE-AC05-96OR22464.

## References

- Haselkorn, M. K., *Insulating Structural Ceramics for High Efficiency, Low Emission Engines*. Department of Energy response to proposal, Notice of Program Interest, Caterpillar Inc, 1996.
- Wachtman, J. B., *Mechanical Properties of Ceramics*. John Wiley and Sons, New York, 1996.
- ASTM C 1161, Standard test method for flexural strength of advanced ceramics at ambient temperature. In *1998 Annual Book of ASTM Standards*, ed. R. F. Allen et al. American Society for Testing and Materials, Philadelphia, PA, 1998, pp. 304–313.
- ASTM C 1421, Standard test method for determination of fracture toughness of advanced ceramics at ambient temperatures. In *1999 Annual Book of ASTM Standards*, ed. R. F. Allen et al. American Society for Testing and Materials, Philadelphia, PA, 1999, pp. 789–823.
- ASTM C 1239, Standard practice for reporting uniaxial strength data and estimating weibull distribution parameters for advanced ceramics. In *1998 Annual Book of ASTM Standards*, ed. R. F. Allen et al. American Society for Testing and Materials, Philadelphia, PA, 1998, pp. 354–371.
- Cuccio, J. C., Brehm, P., Fang, H. T., Hartman, J., Meade, W., Menon, M. N., Peralta, A., Song, J. Z., Strangman, T., Wade, J., Wimmer, J. and Wu, D. C., *Life Prediction Methodology for Ceramic Components of Advanced Heat Engines, Phase I. ORNL/Sub/89-SC674/1*. Oak Ridge National Laboratory, Oak Ridge, TN, 1995.
- ASTM C 1368, Standard test method for determination of slow crack growth parameters of advanced ceramics by constant stress-rate flexural testing at ambient temperatures. In *1998 Annual Book of ASTM Standards*, ed. R. F. Allen et al. American Society for Testing and Materials, Philadelphia, PA, 1998, pp. 688–696.